THE VERTICAL PROFILE OF MARTIAN AEROSOL PARTICLE SIZE.

S.D. Guzewich[1], **M.D. Smith**[2], and **M.J. Wolff**[2], [1]NASA Postdoctoral Fellow, NASA Goddard Space Flight Center, Greenbelt, MD, USA (scott.d.guzewich@nasa.gov), [2]NASA Goddard Space Flight Center, Greenbelt, MD, USA, [3]Space Science Institute, Boulder, CO, USA.

Introduction: During the extended mission of the Mars Reconnaissance Orbiter mission, the Combined Reconnaissance Imaging Spectrometer for Mars (CRISM) has made periodic limb-viewing geometry observations of the atmosphere [1]. These limb scans enable vertical profiles of dust and water ice aerosols to be retrieved with high vertical resolution. [1] described the results of these scans using a retrieval algorithm with a fixed effective radius of 1.5 μm for dust and 2 μm for water ice particles. In this work, we discuss retrievals of the vertical variation of dust and water ice aerosol particle sizes from CRISM limb-viewing observations.

Data and Methods: During a CRISM limb scan, the MRO spacecraft is tilted to allow CRISM to scan upward and downward across the limb from the surface to above 100 km altitude. Sufficient radiance is typically available to enable retrieval of a vertical profile from the near-surface to 50-60 km altitude. The sampling of the CRISM instrument produces pixel resolution of approximately 800 m at the limb tangent point. As part of the retrieval, we further average the central 40 pixels "across track" (parallel to the limb) to increase signal-to-noise ratio and perform a running average of three pixels perpendicular to the limb resulting in a vertical resolution of roughly 3 km.

For limb-geometry observations, the retrieval algorithm must treat the spherical geometry of the observation. This is accomplished through a "pseudo-spherical" approximation that has been validated against a Monte Carlo technique. This technique is orders of magnitude faster than the Monte Carlo technique, while still producing comparable results [1; 2]. The forward radiative transfer model accounts for multiple scattering using the discrete ordinates method.

The retrieval algorithm is provided with a look-up table for extinction coefficients and single-scattering albedos containing 4 distributions of dust particle size (effective radii, r_{eff}, of 0.5 μm, 1.0 μm, 1.5 μm and 2.5 μm) and 4 distributions of water ice particle size (r_{eff} of 0.5 μm, 1.0 μm, 2.0 μm and 4.0 μm). These effective radii were chosen to span a range of values reported in the literature. The effective variance, v_{eff}, for the dust particle size distributions is 0.3 and 0.1 for water ice. Scattering properties for intermediate particle size distributions are found by interpolation between those values. A best fit between observed and computed radiance is accomplished using a Marquardt-Levenberg minimization routine, with the fitted parameters being the dust and water ice particle size and opacity as a function of height above the surface.

Twelve wavelengths are used in the retrieval. These wavelengths were chosen to produce the best discrimination between different particle sizes while considering computational expense. Selected wavelengths are weighted toward the water ice absorption feature near 2800 nm.

The CRISM limb scans began in late MY 29, and approximately 350 atmospheric profiles are included in this study. Most fall in one of two pole-to-pole tracks roughly falling over the Tharis province in the western hemisphere and over Hellas Basin/Syrtis Major in the eastern hemisphere.

Uncertainties in our results source from a number of factors including the pseudo-spherical approximation, choice of parameters (e.g., number of streams) in the algorithm and choice of particle size distributions and associated scattering properties. Our empirical estimate of error in our retrieved particle size is ± 0.25 μm, following Smith et al. [2013].

Results: *Aphelion Cloud Belt:* As identified by [3], we find the Aphelion Cloud Belt (ACB) to be composed of larger water ice particles with a strong gradient of particle size with height, suggesting gravitational sedimentation or changing microphysical conditions over the altitude range of cloud formation. The 30 km altitude is a dividing point between particle sizes greater than 2 μm below this level and less than 2 μm above (Figure 1). Particle sizes increase to near 3 μm at 20 km.

Polar Hood: Because CRISM observations require sunlight, data at high latitudes in local winter is comparatively limited to that in lower latitudes. However, where data is available, some trends are present. During fall and winter in both hemispheres, water ice particle sizes are very uniform throughout the atmospheric column at a size of approximately 1.5 μm.

Dust: The discrete dust layer in the tropics termed the "high altitude tropical dust maximum" by [4] and "lower dust maximum" by [5] shows up clearly in the CRISM retrievals and follows the seasonal cycle described by [5]. Small particle size has been suggested as a possible mechanism to sustain this layer over long time periods.

However, we find that dust particle size is remarkably uniform throughout the Martian atmosphere above the lowest scale height to an altitude of ~40 km (Figure 2). Throughout the year and at most latitudes, the retrieved dust particle size is near 1 μm. Few retrievals are available (or reliable) in the lowest scale height of the atmosphere due to excessive line-of-sight opacity, but those retrievals that are available suggest larger particle sizes (nearer the canonical value of 1.5 μm) in that layer. There is no clear change in particle size within the detached tropical dust layers relative to the surrounding atmosphere. With no clear indication of gravitational sedimentation producing sorting of particle size with height, our work suggests that the atmosphere up to ~40 km altitude is well-mixed on time scales less than the settling time of 1 μm dust particles. For 1 μm dust particles, this time scale ranges from 2-20 sols [6].

References:

[1] Smith, M. D., M. J. Wolff, R. T. Clancy, A. Kleinböhl, and S. L. Murchie (2013), *J. Geophys. Res.Planets*, 118.

[2] Wolff, M. J., et al. (2006), *J. Geophys. Res.*, 111.

[3] Clancy, R. T., M. J. Wolff, and P. R. Christensen (2003), *J. Geophys. Res.*, 108.

[4] Heavens, N. G., M. I. Richardson, A. Kleinböhl, D. M. Kass, D. J. McCleese, W. Abdou, J. L. Benson, J. T. Schofield, J. H. Shirley, and P. M. Wolkenberg (2011), *J. Geophys. Res.*, 116.

[5] Guzewich, S. D., E. R. Talaat, A. D. Toigo, D. W. Waugh, and T. H. McConnochie (2013), *J. Geophys. Res. Planets*, 118.

[6] Kahre, M. A., J. L. Hollingsworth, R. M. Haberle, and J. R. Murphy (2008), *Icarus*, **195**.

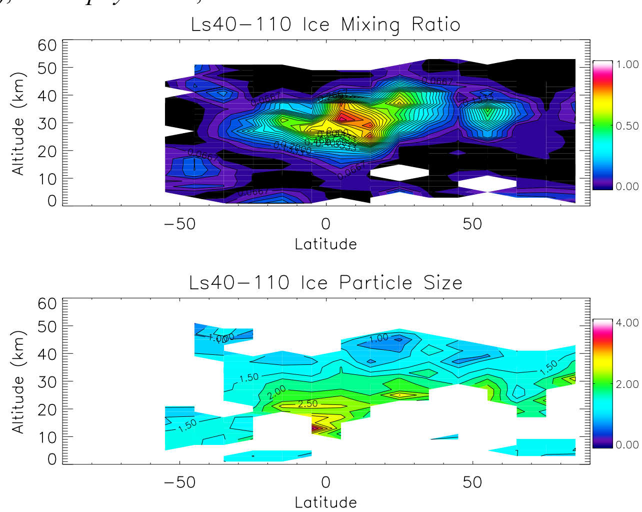

Figure 1. Ice mixing ratio (top, Δτ/mb at 2210 nm wavelength) and effective radius of ice particles (bottom, μm) during the L_s = 40-110° period covering the aphelion cloud belt.

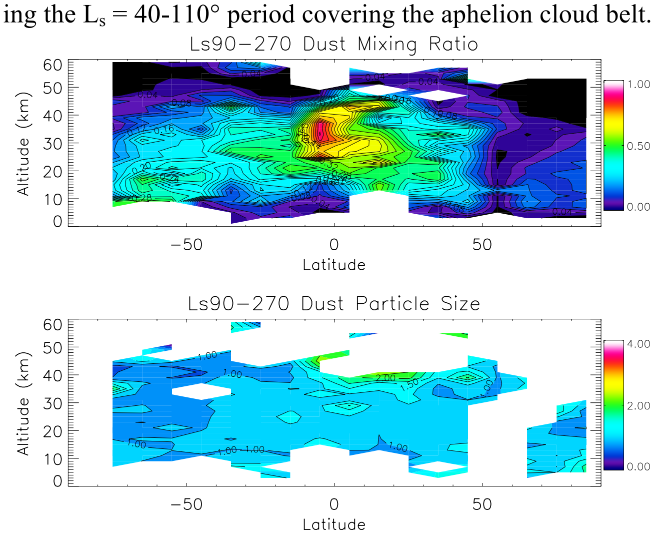

Figure 2. Dust mixing ratio (top, Δτ/mb at 2210 nm wavelength) and effective radius of dust particles (bottom, μm) during the L_s = 90-270° period.